AUGMENTATION OF CONVECTION HEAT TRANSFER FROM A HORIZONTAL CYLINDER IN A VENTED SQUARE ENCLOSURE WITH VARIATION OF LOWER OPENING SIZE

by

Omar M. ALI[a*], Raid A. MAHMOOD[a,b], and Mohammed W. AL-BRIFKANI[c]

[a] Collage of Mechanical Engineering, University of Zakho, Kurdistan Region, Iraq
[b] School of Mechanical and Electrical Engineering, University of Southern Queensland, Queensland, Australia
[c] Mechanical Department, Duhok Technical Institute, Duhok Polytechnic University, Kurdistan Region, Iraq

Original scientific paper
https://doi.org/10.2298/TSCI201119176A

Natural and mixed convection heat transfer from a horizontal cylinder placed in a vented square enclosure has been investigated using numerical method with ANSYS Fluent 16.1 software for laminar and turbulent flow. Navier-Stokes equations and energy equation with standard k-ω transport equation turbulence model have been used to simulate both flow and thermal behaviors. The operating conditions covered a range of the Rayleigh number from 10^3 to 10^6 and the Richardson number range between 0.1 and 100 at variable sizes of the lower open vent with constant upper opening size. The Nusselt numbers, velocity lines and isotherms are presented to display the flow and thermal behaviors. The results displayed that the average Nusselt number is affected by Rayleigh number, Richardson number, enclosure width, and lower opening size. The Nusselt number is enhanced by controlling the lower opening size. The maximum enhancement range for Nusselt number is between 20-85% depending on the Rayleigh number, Richardson number, enclosure width to cylinder diameter, and lower opening size. The velocity lines and isotherms are directly affected by the Rayleigh number, Richardson number, enclosure width to cylinder diameter, and lower opening size.

Key words*: mixed, heat transfer, Richardson number, Rayleigh number, cylinder, enclosure*

Introduction

The forced and natural-convection are the main types of the convection heat transfer. The combination of natural and forced convection that developed together is called mixed convection heat transfer. The forced heat transfer mode is obtained when $Gr/Re^2 << 1$ and $Nu = f(Re, Pr)$. The natural-convection is produced if $Gr/Re^2 >> 1$ and $Nu = f(Gr, Pr)$, and the mixed convection is reached when $Gr/Re^2 \approx 1$, [1, 2]. There are a lot of applications for natural-convection mode enclosed cylinder such as air conditioning systems, solar energy applications, and electronic components cooling [3]. However, the enhancement of the natural-convection heat transfer and its behavior are affected on the applications [4]. Many studies studied the natural-convection from a horizontal cylinder and its enhancement using different fluids such as air [5], water [6], nanofluid [7], and porous medium [8]. The enhancement of heat transfer are

* Corresponding author, e-mail: omar.ali@uoz.edu.krd

studied by some researchers using different methods such as enclosure dimension change [9, 10], magnetic fields [11], or a different medium [12]. Ali *et al*. [7] numerically studied the enhancement of natural-convection heat transfer performance from a cylinder placed in a square enclosure with water-based Cu nanofluid as a transfer medium. The range of the Rayleigh number between 10^4 and 10^6, nanoparticle volume fraction between $0 < \phi \leq 0.2$, and the width of the enclosure to cylinder height ratio, W/H is 2.5. The results revealed that the average Nusselt number increased significantly when the Rayleigh number and nanoparticle volume fraction are increased. Kahwaji *et al*. [13] provided an experimental study to determine the Nusselt number in natural-convection heat transfer from a square cross-sectional cylinder located in a vented enclosure with the range of $10^7 \leq \mathrm{Ra} \leq 6.6 \cdot 10^7$, $2 \leq W/D \leq 4$, $0.25 \leq O/D \leq 4$. The results displayed Nusselt number increased proportionally with the vent size at low enclosure widths and it is inversely proportional with vent size for high enclosure widths. Rahmati and Tahery [14] investigated the effect of Rayleigh number, obstacle dimension, nanofluid volume fraction, cavity dimensions, surface ratio and various models for thermal conductivity coefficient and viscosity coefficient on Nusselt number and heat transfer around hot obstacles in an enclosure for laminar natural-convection of water-TiO_2 nanofluid using the lattice Boltzmann method. The results indicated that the average Nusselt number increased with the increase in Rayleigh number and volume fraction. The obstacle and cavity dimensions have an influence on the flow and thermal behaviors. Mixed convection heat transfer has been studied by a number of researchers such as [2, 15-20]. Pourmahmoud *et al*. [15] investigated numerically the laminar mixed convection in a cavity employed water-Al_2O_3, water-Cu or water-TiO_2 nanofluids as medium work. The top and bottom walls are adiabatic and the vertical walls are isothermal with different temperatures. The range of the parameters are Rayleigh number between 10^3-10^6 and solid concentration between 0-0.2 at constant Reynolds and Prandtl numbers. For all Rayleigh numbers, the average Nusselt number increased as the nanoparticles volume fraction is increased and the heat transfer is enhanced as thermal conductivity coefficient of nanoparticles is increased. The maximum values are obtained when using Cu nanoparticles. Mahmoodi [17] studied the mixed convection heat transfer in a 3-D ventilated cavity numerically with finite volume method. The results indicated that the flow intensity and the heat transfer rate are enhanced by an optimal choice of the Reynolds and Richardson numbers, relative height of the openings and relative width of the openings. Mixed convection heat transfer characteristics from a square cylinders at various operating conditions have been studied by [18]. They reported that for fixed lateral distance between the cylinders, maximum heat transfer was found to occur at an incident angle of 45°. Karimi *et al.* [2] studied numerically the steady-state mixed convection around two heated horizontal cylinders at the middle of the square enclosure height. The results indicated that the heat transfer rates from the heated cylinders and the dimensionless fluid temperature in the enclosure increased with increasing Richardson number and cylinder diameter. The average Nusselt number and non-dimensional temperature variation trends were different when the Reynolds number increased. The left cylinder was less affected by the inlet flow than right one. A number of studies have used CFD to predict the heat transfer and flow behavior around heated cylinder and to obtain optimum design. Fourar *et al*. [21] presented a CFD simulation analyze the heat transfer from the horizontal cylinder surrounded by fins. The results displayed that the eccentricity effect is appeared with small fin diameter having high thermal conductivity materials and thick fins produce best heat transfer. Graževičius *et al*. [22] performed a CFD investigation in two-phase (water and air) natural-convection and thermal stratification phenomena with conjugate heat transfer in the rectangular enclosure. The authors reported that the natural-convection was formed in the region above the heater rod (horizontal cylinder) and the water was thermally stratified in the region below the heater rod.

A number of studies have dealt with the enhancement of the natural and mixed convection heat transfer from a cylinder using different methods. However, in the shrouded cylinder, two symmetrical openings at the lower and upper ends of the enclosure are used for previous studies and the effect of the lower opening size on heat transfer enhancement has not been studied experimentally or numerically. So, the studies deal with only natural-convection heat transfer and the effect of mixed convection heat transfer is not included. The present work includes the numerical investigation of the natural and mixed convection heat transfer from the horizontal cylinder in a symmetrical open square enclosure. The governing equations were solved using the finite volume method. Two enclosure widths W/D = 2.5 and 4, Raynolds number range between 10^3-10^6 and lower opening size range between O_1/W = 0.2 to 1 for W/D = 2.5 and 0.125-1 for W/D = 4 at constant O_2/W are used. The study includes an investigation determine the enhancement of heat transfer from the horizontal cylinder in a vented enclosure and the behaviors of the velocity distribution and isotherms. The numerical method results will be compared with experiments, Ali [4].

Mathematical formulation and numerical method

Theoretical formulation

Figure 1 presents the schematic view of the experimental rig for the horizontal cylinder placed inside a square enclosure. The assumptions of the present study are 2-D, steady-state and constant properties for laminar and turbulent flows. The cylinder diameter is 5 cm using two different enclosure widths 12.5 cm and 20 cm. The cylinder is placed in the middle of the enclosure. The upper opening size is constant (2.5 cm) while the lower opening size between 2.5 cm to full opening size for both enclosure widths.

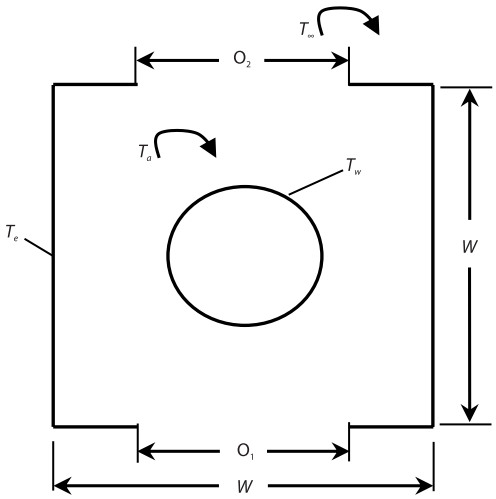

Figure 1. Configuration of cylinder and enclosure

Governing equations

The mathematical model based upon the flow is incompressible, steady, turbulent and 2-D. The Navier-Stokes and the energy equations have been employed to describe and predict the hydrodynamic and heat fields [20, 23]. The gravitational acceleration has been acted in the negative direction of the flow. The standard k-ω transport equation turbulence model is used to predict the eddy viscosity [2]:

$$\frac{\partial u}{\partial x}+\frac{\partial v}{\partial y}=0 \tag{1}$$

$$u\frac{\partial u}{\partial x}+v\frac{\partial u}{\partial y}=-\frac{1}{\rho}\frac{\partial p}{\partial x}+\left(\nu+\nu_t\right)\left(\frac{\partial^2 u}{\partial x^2}+\frac{\partial^2 u}{\partial y^2}\right) \tag{2}$$

$$u\frac{\partial v}{\partial x}+v\frac{\partial v}{\partial y}=-\frac{1}{\rho}\frac{\partial p}{\partial y}+\left(\nu+\nu_t\right)\left(\frac{\partial^2 v}{\partial x^2}+\frac{\partial^2 v}{\partial y^2}\right)+\mathrm{g}\beta\left(T-T_m\right) \tag{3}$$

The energy equation can be solved for the heat transfer [24]:

$$u\frac{\partial T}{\partial x}+v\frac{\partial T}{\partial y}=\left(\frac{\nu}{\mathrm{Pr}}+\frac{\nu_t}{\sigma_T}\right)\left(\frac{\partial^2 T}{\partial x^2}+\frac{\partial^2 T}{\partial y^2}\right) \tag{4}$$

The Richardson number is a dimensionless ratio between the buoyant production and shear production. It can be used to indicate the formation of turbulent and dynamic stability [25]. The Richardson number can be estimated [2]:

$$\mathrm{Ri}=\frac{\mathrm{g}\beta D\left(T_w-T_\infty\right)}{u_i^2}=\frac{\mathrm{Gr}}{\mathrm{Re}^2}$$

where the Gr is Grashof number, Re – the Reynolds number, u_i – the flow velocity, β – the volume expansion coefficient, g – the gravitational acceleration, T_w and T are the cylinder surface and internal fluid temperature:

$$\mathrm{Gr}=\frac{\mathrm{g}\beta\left(T_w-T_\infty\right)D^3}{\nu^2},\ \mathrm{Re}=\frac{\rho\, u_i\, D}{\mu}$$

The standard k-ω turbulence model is used for two transport equations, one for the turbulent kinetic energy, k, and one for the turbulent specific dissipation, ω. The model is chosen because it is numerically very stable, as it tends to produce converged solutions more rapidly than the k-ε models [26]. The stress tensor is computed from the eddy-viscosity concept k-equation:

$$\rho\frac{\partial}{\partial x_j}\left(u_j k\right)=\frac{\partial}{\partial x_j}\left[\left(\frac{\mu_t}{\sigma_k}+\mu\right)\left(\frac{\partial k}{\partial x_j}\right)\right]+P_k-\beta'\rho k\omega+P_{kb} \tag{5}$$

ω-equation:

$$\rho\frac{\partial}{\partial x_j}\left(u_j\omega\right)=\frac{\partial}{\partial x_j}\left[\left(\frac{\mu_t}{\sigma_\omega}+\mu\right)\left(\frac{\partial\omega}{\partial x_j}\right)\right]+\alpha\frac{\omega}{k}P_k-\beta\rho\omega^2+P_{\omega b} \tag{6}$$

The constants for the previous equation are represented by $\beta' = 0.09$, $\alpha = 5/9$, $\beta = 0.075$, $\sigma_k = 2$, and $\sigma_\omega = 2$.

The P_k is the turbulence production due to viscous forces, and is modeled using:

$$P_k=\mu_t\left[\frac{\partial u_i}{\partial x_j}+\frac{\partial u_j}{\partial x_i}\right]\frac{\partial u_i}{\partial x_j}-\frac{2}{3}\frac{\partial u_k}{\partial x_k}\left(3\mu_t\frac{\partial u_k}{\partial x_k}+\rho k\right) \tag{7}$$

Boundary conditions

The boundary conditions to predict the flow and thermal behavior for the convection mode were applied. The boundary conditions can be summarized in the non-dimensional form:

- The $T = 1$, U, $V = 0$ at the cylinder's surface.
- The $T = 0$, U, $V = 0$ at the enclosure's walls.
- The $T = T_{\mathrm{amb}}$, $U = 0$, $V =$ constant at lower opening.

Convective boundary condition at upper opening, pressure = 0.

Nusselt number

The average Nusselt number of the cylinder surface is calculated from the integration:

$$\mathrm{Nu}_{\mathrm{ave}} = \frac{h_{\mathrm{ave}} D}{k} = -\frac{1}{2\pi}\int_0^{2\pi} \frac{\partial \theta}{\partial n} \tag{8}$$

where h_{ave} presents the average convection heat transfer from the cylinder and k – the thermal conductivity of the air.

Numerical method

The governing equations are solved numerically using ANSYS, FLUENT 16.1 software. The Boussinesq approximation is assumed during the solution of the momentum equation. The properties of the fluid in the medium are based on the average temperature of the cylinder surface and the ambient air. The pressure velocity coupling, SIMPLE algorithm has been used with second order upwind scheme for the discretization of momentum, energy and turbulence model equations. A convergence criterion of 10^{-6} is used as residuals of the continuity, momentum energy and k-ω equations.

Grid independence study

The mesh was generated for the geometry using ANSYS meshing method with hexahedral cell type and assessed to select the best mesh size and number for the simulations, fig. 2. Four different mesh numbers were used: 8309, 14663, 39749, and 151120 for $\mathrm{Ra} = 5 \cdot 10^4$ with geometry $W/D = 4$, $O_1/W = 0.5$, and $O_2/W = 0.125$. The Nusselt number values were obtained for each mesh Case 10.61, 10.43, 10.38, and 10.3, respectively. The value of the Nusselt number from the numerical method was compared with the experimental value that was obtained from the previous study. The comparison showed that there was no significant change between the numerical and the experimental results. The mesh number 14663 is selected because the percentage error is low as compared with experimental results. The employment of large amount of mesh at high Rayleigh number, the solution become divergent.

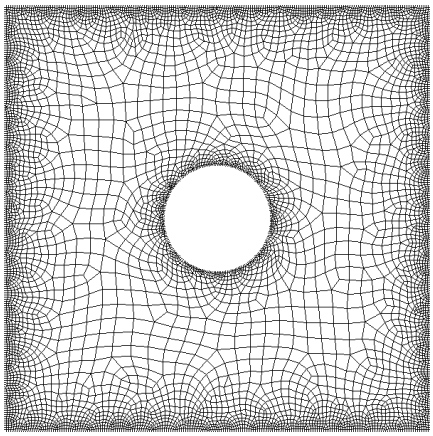

Figure 2. Typical grid distributions in the computational domain

Code validation

The validation of the present CFD code is checked by comparing the present CFD results with previous experimental results. The validated problem is the natural-convection induced using two enclosure widths. The obtained numerical solution for a single cylinder embedded in an enclosure $W/D = 2.5$ and 4 and symmetrical opening sizes equal to 2.5 cm has been compared with experimental result that presented by Ali [4]. The comparison has been obtained under the same geometry, boundary conditions and other parameters of the experimental test. The comparisons for two cases are presented in terms of the average Nusselt number as shown in fig. 3. The results show that the Nusselt number has been increased when the Rayleigh number is increased. The comparisons in fig. 3 show very good agreement between the present

numerical and previous experimental results, where the maximum percentage error between both results is about 3.5%.

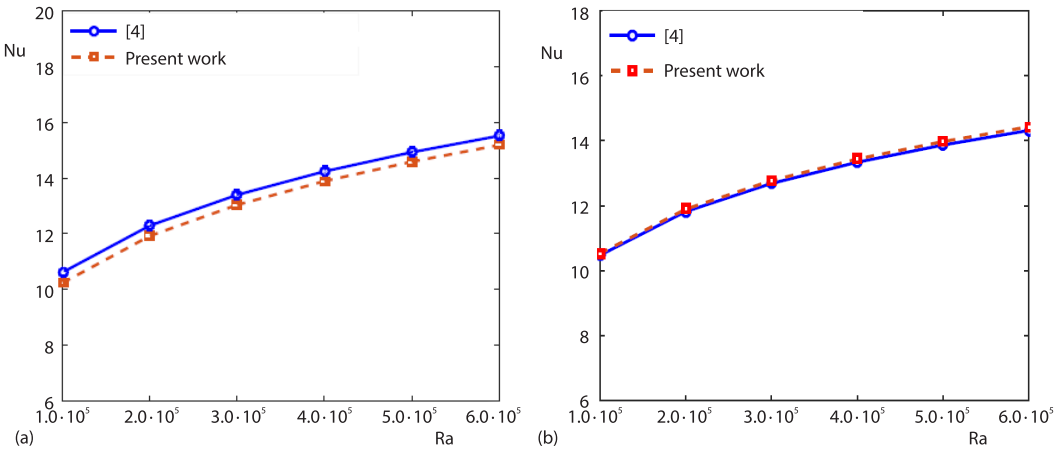

Figure 3. Comparisons between the CFD and previous experimental work; (a) $W/D = 4$, $O_1/W = O_2/W = 0.125$ and (b) $W/D = 2.5$ cm, $O_1/W = O_2/W = 0.2$

Results and discussion

The results of the present numerical work involve the natural and mixed convection heat transfer from heated cylinder induced in a cold square enclosure with constant upper opening size and variable lower opening sizes will be presenting in this section. Air has been employed as a working fluid inside the enclosure which surrounded the cylinder. According on the dimensionless variables, the studied parameters are ranged:

- Dimensionless of enclosure width length (W/D): 2.5, 4
- Dimensionless of lower opening size (O_1/W): 0.125-1.
- Dimensionless of upper opening size (O_2/W): 0.2 for $W/D = 2.5$ and 0.125 for $W/D = 4$.
- Rayleigh number: 103-106.
- Richardson number: 0.1-100.

The influence of a wide range of Rayleigh numbers, Richardson numbers, lower opening size and enclosure width on the temperature and velocity distributions have been investigated and discussed to demonstrate the behaviors of the thermal and hydrodynamic flow fields. Also, the impact of these parameters on the average Nusselt numbers behaviors have been illustrated in the results and discussions section.

The mass-flowrate entering the opening size was increased with the increase of the O_1/W size because the inlet velocity was constant for each Rayleigh numbers. The flow strength enhanced and the Reynolds number increased with the increase of the opening size that leads to a decrease in the Richardson number, and the mixed convection mode is obtained. The Richardson number values are changed with the change of different enclosure widths W/D, lower opening size O_1/W and Rayleigh number at constant upper opening size O_2/W. It is noted that the Richardson number have been large values for $O_1/W = 0.125$ and 0.2 at $W/D = 2.5$ and 4, respectively, for different Rayleigh number, which ensures the mode of heat transfer is natural-convection. The Richardson number values are between 0.1 and 6 for $O_1/W > 0.5$, therefore, the mode of heat transfer is mixed convection for these cases. The flow become turbulent at high Rayleigh numbervalues with low Richardson number.

Effects of pertinent parameters on Nusselt number

The variations of the average Nusselt numbers for various relevant parameters are presented in figs. 4-8.

Figure 4 illustrates the variations of average Nusselt number as a function of Rayleigh number for two W/D sizes at low O_1/W. The average Nusselt number has been increased with increasing in Rayleigh number for all cases. The average Nusselt number in a vented enclosure increases as compared with those of the free cylinder. The average Nusselt number enhancement for W/D = 4 is larger than those for W/D = 2.5 at low and medium Rayleigh number, but the enhancements have same values at high Rayleigh number. The Richardson number values for this case have been recorded as very large which indicate that the heat transfer mode was natural-convection. The enhancement percentage of average Nusselt number have been ranged between 20-40% as compared with those of free cylinder.

Figure 5 presents the variation of the average Nusselt with the Rayleigh number when O_1/W = 0.5 at W/D = 2.5 and O_1/W = 0.25 at W/D = 4. The figure shows the average Nusselt number increased as Rayleigh number is increased. The Nusselt number enhancement for Ra < 10^5 at W/D = 4 is larger than Nusselt number enhancement at W/D = 2.5, while, the Nusselt number have similar values at high Rayleigh number. It is indicted that the dominant convection mode is mixed convection at low Rayleigh number because the Richardson number value was less than 10. The convection mode become natural-convection at Ra > 2000. The maximum increasing percentage was achieved for Nusselt number was 50% at W/D = 4 and about 20% as compared with those of free cylinder.

Figure 6 shows the variation of average Nusselt number with Rayleigh number at O_1/W = 1 for two W/D. The average Nusselt number is increased with the increase of Rayleigh number at both W/D. The Nusselt number increase for all Rayleigh number at

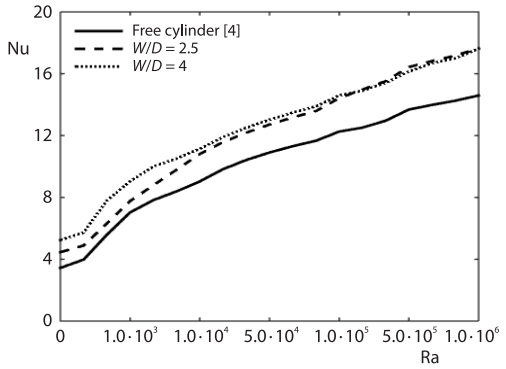

Figure 4. Enhancement of the Nusselt number for different Rayleigh number due to enclosure width variation for $O_1/W = O_2/W$ = 0.2 at W/D = 2.5 and $O_1/W = O_2/W$ = 0.125 at W/D = 4

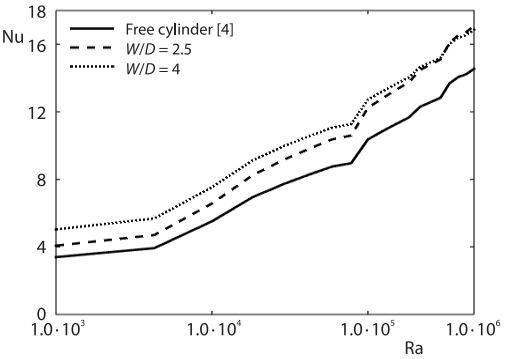

Figure 5. Enhancement of the Nusselt number for different Rayleigh number due to enclosure width variation for O_1/W = 0.5, O_2/W = 0.2 at W/D = 2.5 and O_1/W = 0.25, O_2/W = 0.125 at W/D =4

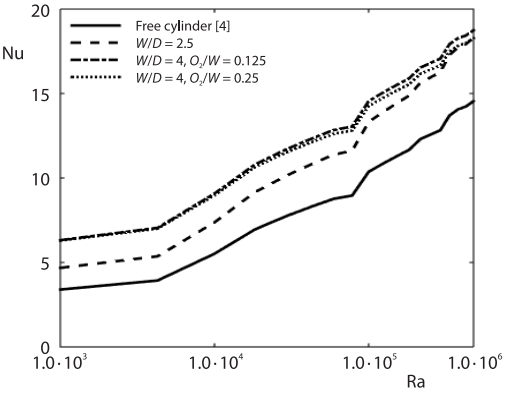

Figure 6. Enhancement of the Nusselt number for different Rayleigh numbers due to enclosure width variation for complete lower opening size

$W/D = 4$ is greater than those at $W/D = 2.5$ as compared with Nusselt number at free cylinder. The enhancement percentage depends on the Rayleigh number and W/D, it is varied between 40% at $W/D = 2.5$% to 80% at $W/D = 4$ at $Ra < 10^4$. The increase percentage range in the Nusselt number between 30-35% at $W/D = 2.5$ and $10^4 \leq Ra \leq 10^5$, while the percentage increase in the Nusselt number between 45-55% at $10^4 \leq Ra \leq 10^5$ and 30-40% at $Ra > 10^5$ for $W/D = 4$ as compared with those of free cylinder. The O_2/W size have not influence on the Nusselt number enhancement at $W/D = 4$ as displayed in figure. The Richardson number values are ranged between 0.1 and 3.5 depending on the Rayleigh number and W/D due to an increase in the fluid velocity and Reynolds number which indicated that the heat transfer mode is the mixed convection.

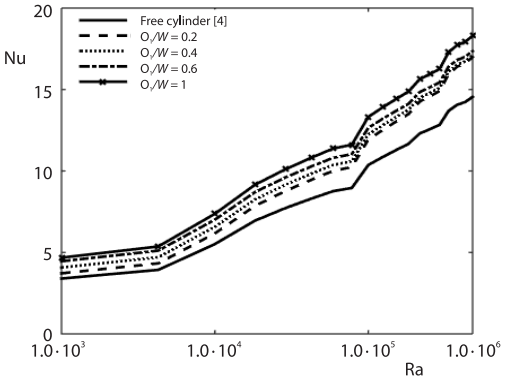

Figure 7. Enhancement of the Nusselt number for different Rayleigh numbers due to lower opening sizes for W/D =2.5

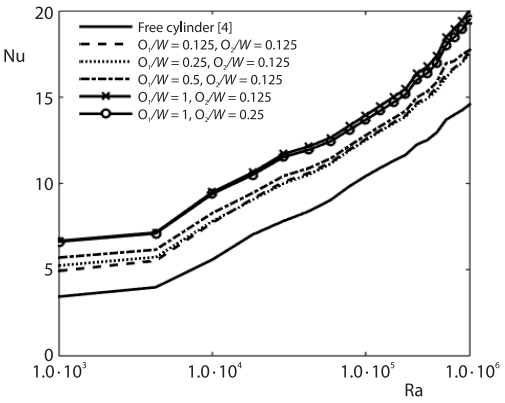

Figure 8. Enhancement of Nusselt number for different Rayleigh numbers due to lower opening sizes for $W/D = 4$

Figure 7 illustrates the variation of average Nusselt number with Rayleigh number at different O_1/W and $W/D = 2.5$. The average Nusselt number increases with Rayleigh number for all O_1/W. The average Nusselt number increases with the increase of O_1/W for all Rayleigh number values. The average enhancement of the Nusselt number was recorded between 15% and 30% when the lower opening vent was fully opened. The maximum increase percentage was 38% at $Ra = 10^3$ and fully O_1/W and it decreases to 30-35% at Rayleigh number between 10^4 and 10^5 and $O_1/W = 1$ as compared with those of free cylinder. The natural-convection heat transfer is the dominant mode for low O_1/W due to high Richardson number, while the mixed convection heat transfer is the governed mode for high O_1/W because the Richardson range between 1-9 that obtained from high fluid velocity around the cylinder.

Figure 8 represents variation of average Nusselt number with Rayleigh number at different O_1/W and $W/D = 4$. The average Nusselt number enhances as Rayleigh number is increased for all O_1/W. The average Nusselt number increases with the increase in Rayleigh number for all O_1/W. The enhancement percentage of the average Nusselt number is ranged between 18% at $O_1/W = 0.125$% and 85% at $O_1/W = 1$. The natural-convection heat transfer is the dominant mode at low O_1/W, while the forced convection was observed at high O_1/W due to the increase in flow velocity and Reynolds number, which lead to a decrease in Richardson number values.

Effects of pertinent parameters on isotherms and streamlines

The influence of lower opening size on the velocity and temperature distributions have been illustrated for a range of opening vent values O_1/W between 0.2-1 for $W/D = 2.5$ and 0.125-1 for $W/D = 4$ with various Rayleigh number values as shown in figs. 9-12. The velocity

and isotherms are symmetrical around the centerline of y-axis of the enclosure for all O_1/W and Rayleigh number values. The Richardson number values are obtained due to the variation of Reynolds number and Rayleigh number for each case. Figure 9 presents the stream velocity distribution for the case $W/D = 2.5$, the flow velocity is increased with the increase of Rayleigh number and O_1/W. For $O_1/W = 0.2$, the flow velocity is relatively low and the hydrodynamic boundary-layer is thick at Ra = 10^3. When the Rayleigh number is increased to 10^5 and 10^6, the vortices are appeared at the upper surfaces of the enclosure, the flow velocity and Reynolds number values are increased, which lead to a decrease in Richardson number values, but the values remain more than 20 and ensures that the mode of heat transfer is natural-convection. For $O_1/W = 0.6$, the mass-flowrate is increased due to the increase in lower opening area, the flow velocity become more for all Rayleigh number and the Reynolds number values are increased which led to a decrease in Richardson number values between 2-9. The mode of heat transfer become mixed but the contribution of natural-convection heat transfer remains high as compared with those of forced convection heat transfer. As O_1/W is increased to 1 (full opening size), the mass-flow rate is increased more and the Richardson number values are reduced to a range between 1 at low Rayleigh number and 5 at high Rayleigh number.

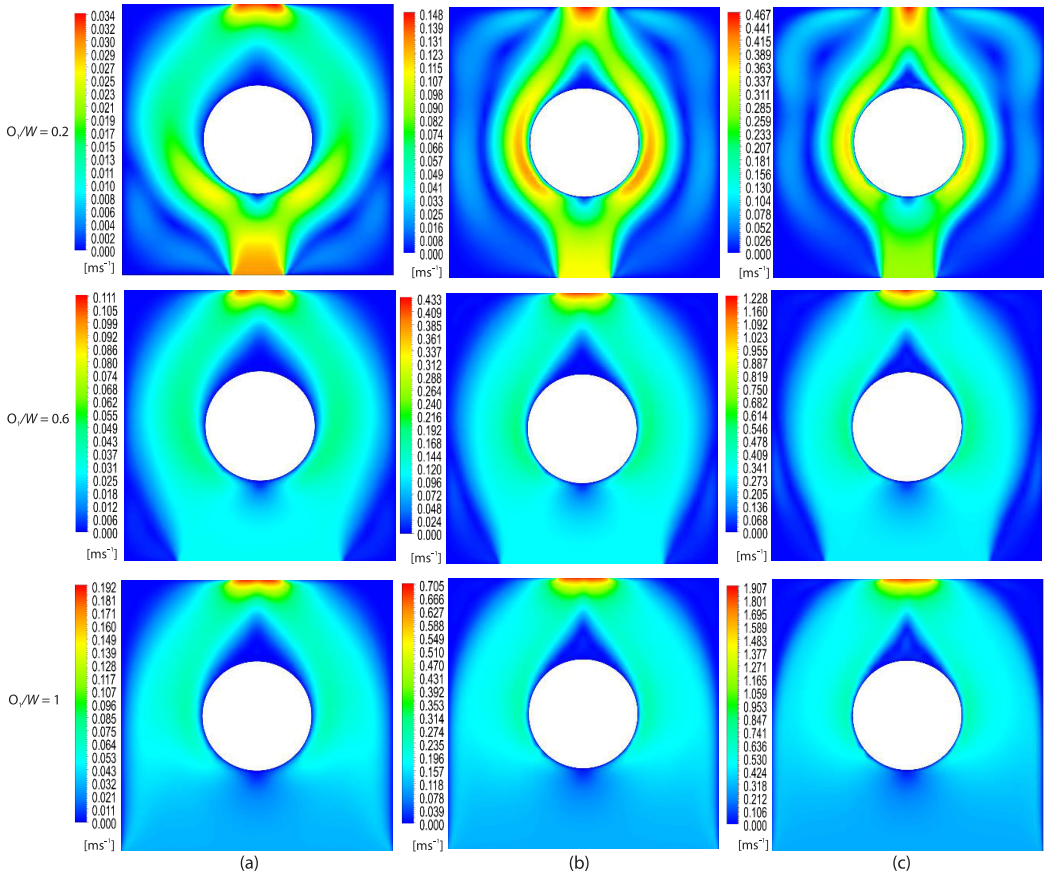

Figure 9. Velocity distribution around the cylinder at $W/D = 2.5$, $O_2/W = 0.2$ and different lower opening sizes; (a) Ra = 10^3, (b) Ra = 10^5, and (c) Ra = 10^6

Figure 10 represents the temperature distribution for case W/D = 2.5 with different Rayleigh number and O_1/W sizes. For O_1/W = 0.2, the isotherms shape displayed that the conduction heat transfer is the dominant mode at Ra = 10^3, then the strength of convection heat transfer become more as Rayleigh number is increased and the thermal boundary-layer thickness around the cylinder is decreased. A thermal plume appears at Ra = 10^3 around the cylinder and covers most of the space between the cylinder and the enclosure. Three thermal plumes are appeared at upper and sides of the cylinder at Ra = 10^5. The sided thermal plumes are disappeared at Ra = 10^6 and the thermal plume above the cylinder directs toward the upper opening size due to the strength of the convection heat transfer. The shapes of the isotherms are changed when the O_1/W is increased to 0.6. At Ra = 10^3, the thickness of the thermal plume around the cylinder is reduced and the thermal boundary-layer around the cylinder become thinner as compared with those for low O_1/W. As Rayleigh number is increased to 10^5, the convection heat transfer becomes the governed mode due to the shape of the isotherms and the thermal boundary-layer around the cylinder become thinner. As Ra = 10^6, the thermal boundary-layer thickness and thermal plume width above the cylinder are decreased. For full opening size, the thermal boundary-layer thickness around the cylinder is decreased more and the influence of the convection heat transfer is increased as displayed from the temperature distribution. Small changes are appeared at Ra = 10^5 and 10^6 as compared with those of O_1/W = 0.6. The width of the thermal plume and thermal boundary-layer thickness around the cylinder become more.

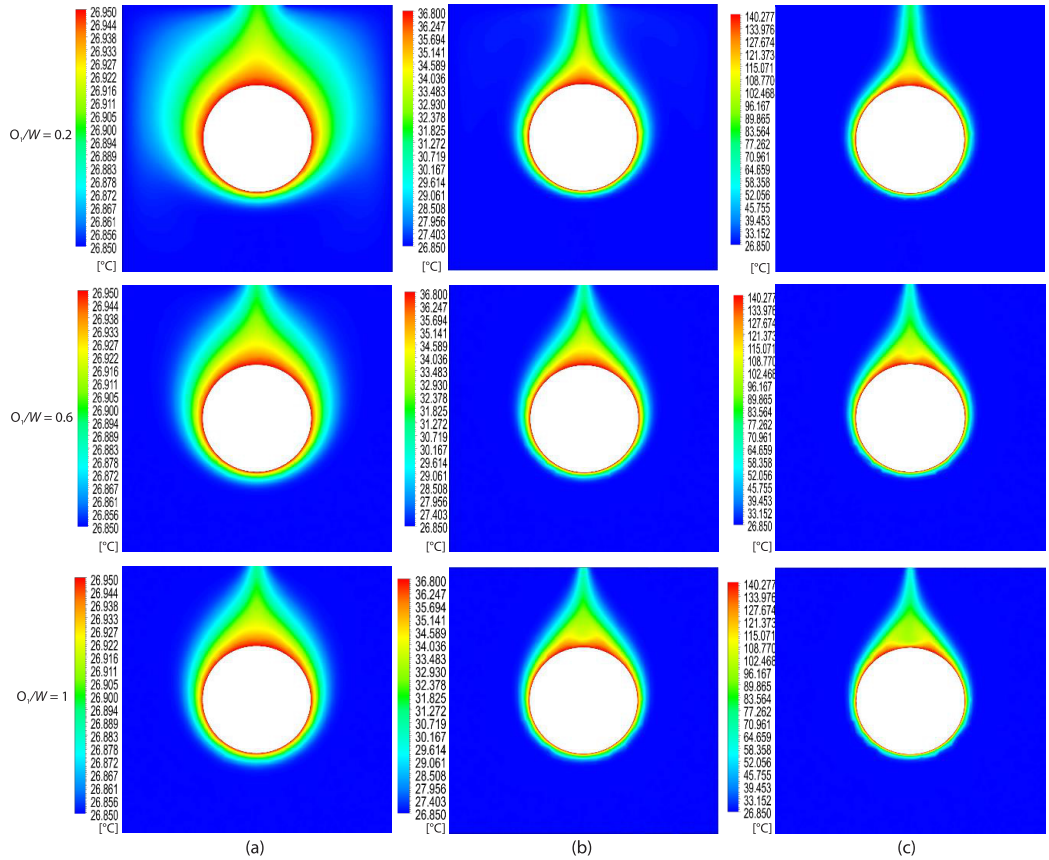

Figure 10. Temperature distribution around the cylinder at W/D = 2.5, O_2/W = 0.2 and different lower opening sizes; (a) Ra = 10^3, (b) Ra = 10^5, and (c) Ra = 10^6

Figure 11 shows the velocity distributions for W/D = 4 case with different sizes of O_1/W and a wide range of Rayleigh number. For O_1/W =0.125, the value of the velocity around the cylinder is relatively low at Ra = 10^3 and it is enhanced when the Rayleigh number is increased. The velocity value is increased as compared with those for the case W/D = 2.5. The velocity lines are appeared as thin layer introduces from the lower vent and exited from the upper vent and passes around the cylinder. Two small vortices are appeared at the sides of the enclosure far from the cylinder. As Rayleigh number is increased, the vortices are appeared beneath the upper surfaces of the enclosure and the strength of these vortices become more as Ra = 10^6. The Richardson number values between around 10 at low Rayleigh number and around 100 at medium and high Rayleigh number, therefore, the heat transfer mode is mixed at low Rayleigh number and natural-convection heat transfer at medium and high Rayleigh number. As O_1/W is increased, the vortices are disappeared and the flow velocity is increased around and above the circular cylinder. For O_1/W = 0.6, the mass-flow rate is increased and the flow velocity is increased, then the Reynolds number is increased, therefore, the Richardson number values are decreased to about 1-2 at low and medium Rayleigh number and 4-5 at high Rayleigh number. The effect of natural and forced convection are equal at low and medium Rayleigh number, while the influence of the natural-convection is enhanced at high Rayleigh number. As O_1/W = 1, the flow velocity is increased more due to high mass-flow rate from the lower

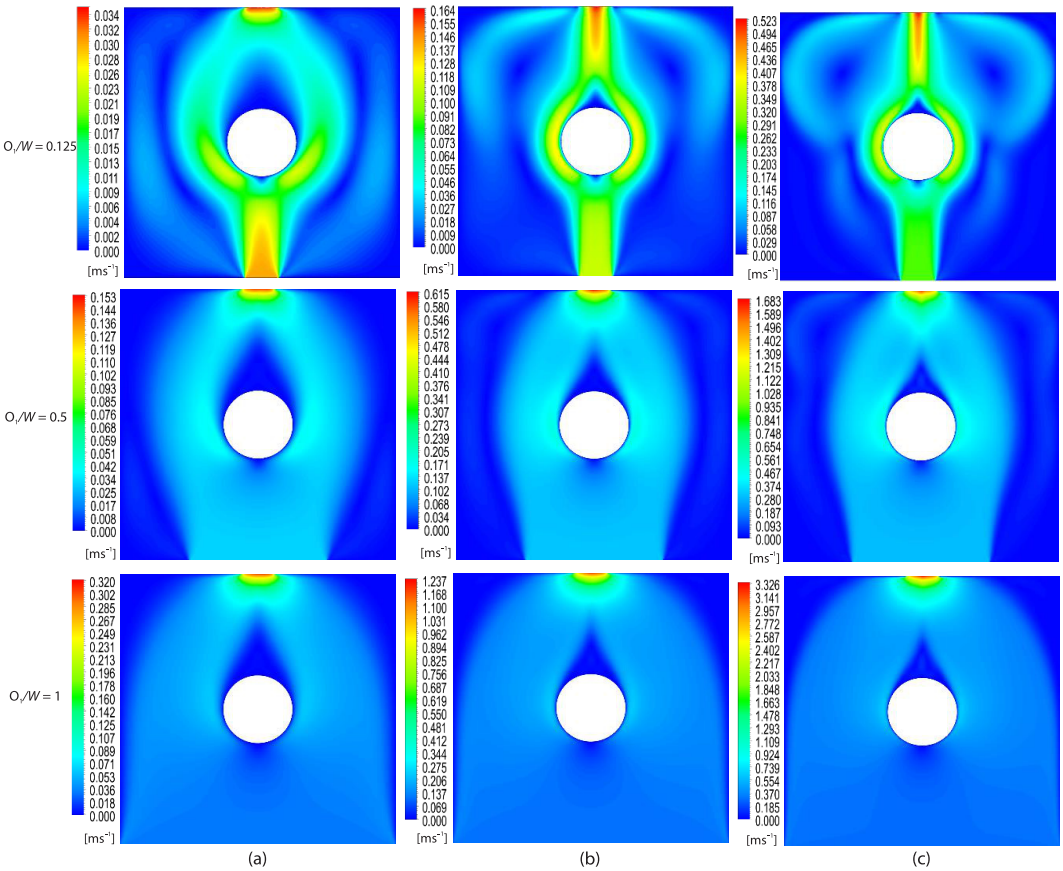

Figure 11. Velocity distribution around the cylinder at W/D = 4, O_2/W = 0.125 and different lower opening sizes; (a) Ra = 10^3, (b) Ra = 10^5, and (c) Ra = 10^6

opening, the Reynolds number values are increased and the Ricardson values are decreased. The range of Richardson number between 0.1 at low and high Rayleigh number values and 1 at high Rayleigh number values, which ensure the dominant mode for low and medium Rayleigh number is the forced convection heat transfer and equal influence of natural and forced for high Rayleigh number.

Figure 12 represents the temperature distributions for the $W/D = 4$ with different range of Rayleigh number and O_1/W. The conduction heat transfer is a dominant mode when the Rayleigh number equals 10^3 and $O_1/W = 0.125$. The strength of the conduction heat transfer is reduced and the convection heat transfer mode become more as Rayleigh number is increased. Thermal plumes appear at sides and above the circular cylinder. As Rayleigh number is increased to 10^5, two thermal plumes appear under the upper surfaces and the thickness of thermal boundary-layer around the cylinder is decreased due to high values of flow velocity, therefore, the convection heat transfer is the governed mode. For $O_1/W = 0.5$, the contribution of the convection heat transfer is increased at Ra = 10^3. The thickness of the thermal boundary-layer decreases as compared with those of $W/D = 2.5$. The thermal boundary-layer thickness around the cylinder decreases and the width of thermal plume decreases as Rayleigh number is increased. For full opening size, the isotherms shapes remain unchanged as those for $O_1/W = 0.6$ but the effect of forced convection become more as discussed previously.

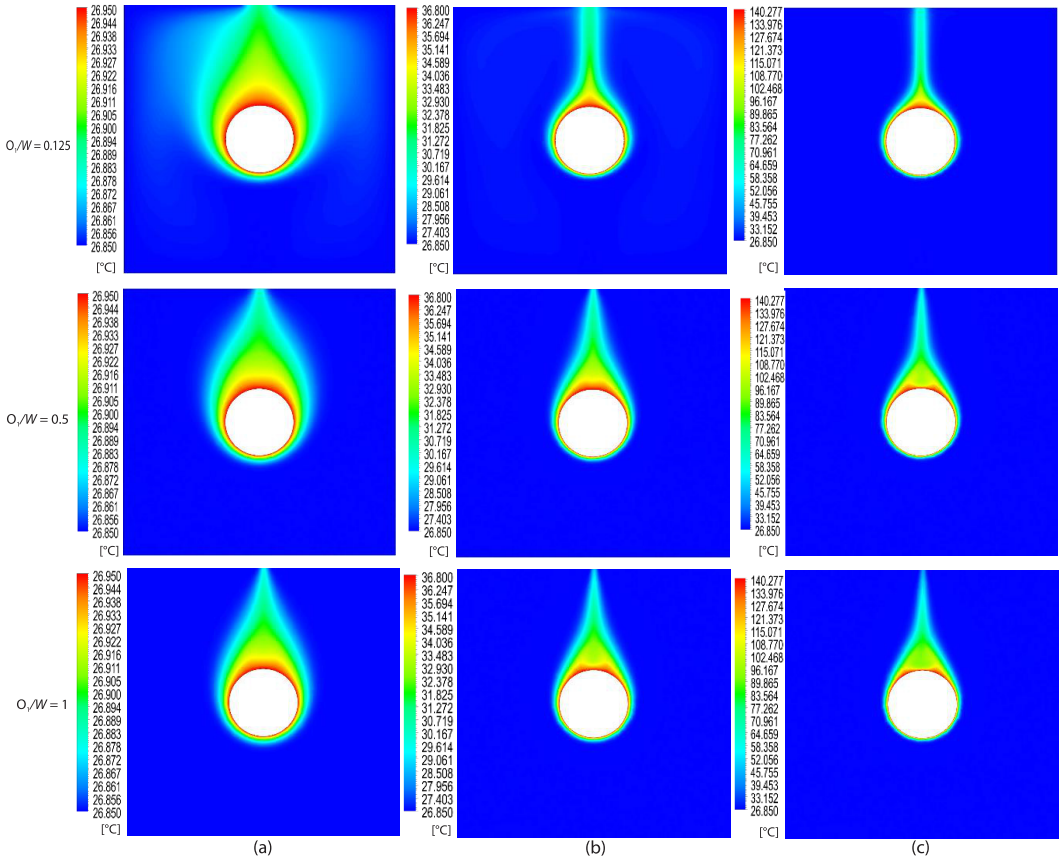

Figure 12. Temperature distribution around the cylinder at $W/D = 4$, $O_2/W = 0.125$ and different lower opening sizes: (a) Ra = 10^3, (b) Ra = 10^5, and (c) Ra = 10^6

Conclusions

The present numerical work involves natural and mixed convection induced by horizontal heated cylinder placed inside a cold square enclosure with two openings at lower and upper surfaces of the enclosure. The mathematical model consisting of Navier-Stokes, energy equation and standard k-ω transport equation model which have used to present the behaviors of fluid-flow and heat transfer fields. The flow has been assumed steady, incompressible, constant thermophysical properties except the density and laminar or turbulent flow depended on the studied parameters. A CFD software package ANSYS FLUENT 16.1, based on finite volume method, has been used to solve the governing equations. The studied parameters have covered a wide range of lower opening size (O_1/W), Rayleigh number and Richardson number ranging from 0.125 (partial opening) to 1 (full opening), from 10^3-10^6, from 0.1-100, respectively. Two enclosure width to cylinder diameter ratio has been used at W/D = 2.5 and 4. The numerical results have been validated against previous experimental results and they indicated very good agreement between them. The results have been presented in terms of velocity, temperature contour lines, local and average Nusselt number. The results of present work may be concluded.

- The findings display that the lower opening size has a considerable influence on the behavior of velocity distributions and appearance of vortices inside the enclosure. For O_1/W = 0.2 and 0.125 (partial opening case), the shape of vortices above the cylinder in the flow field has been varied with the increase in Rayleigh number due to the impact of upper surface of the enclosure, where this effect is released with the case of full opening size.
- The lower opening size, enclosure width and Rayleigh number have significant effect on the temperature distribution above the heated cylinder. The conduction heat transfer is the dominant mode for low Rayleigh number at O_1/W = 0.2 and W/D = 2.5. The effect of convection heat transfer become more as O_1/W and W/D are increased.
- The lower opening size has a considerable effect on the mixed convection heat transfer. The Richardson number for low O_1/W is high and it is increased as O_1/W is increased due to high mass-flowrate.
- The enclosure width has a significant effect on the mixed convection heat transfer. The Richardson number for low O_1/W is high which ensure that the natural-convection heat transfer is the dominant mode, while, it is increased as O_1/W is increased due to high mass-flow rate which the forced convection is the effective mode.
- As Rayleigh number is increased, the thickness of thermal boundary-layer has been decreased depending on the Richardson number value. The values of Richardson number depended on the lower opening size and enclosure width.
- The results display that the average Nusselt number from the cylinder surfaces has been gradually increased with increasing in Rayleigh number, Richardson number, O_1/W, and W/D. The heat transfer enhancement percentage between 20% and 85% as compared with those for free cylinder. The increase in Nusselt number due to the variation of O_1/W at W/D = 4 is larger than those of W/D = 2.5.
- The effect of the upper opening size on the Nusselt results is very low.

Acknowledgment

Authors acknowledge and thank University of Zakho for their support to complete this work.

Nomenclature

D – cylinder diameter, [m]
Gr – Grashof number
g – gravitational acceleration, [ms^{-2}]
H – convection heat transfer coefficient, [Wm^{-2}K^{-1}]
k – thermal conductivity coefficient for air, [Wm^{-1}K^{-1}]
Nu – Nusselt number, [–]
O_1 – lower opening size, [m]
O_2 – upper opening size, [m]
P – dimensionless pressure, [–]
Pr – Prandtl number, [–]
Ra – Rayleigh number, [–]
Re – Reynolds number, [–]
Ri – Richardson number, [–]
T – temperature, [°C]
u – dimensional velocity, [ms^{-1}]
V – dimensional velocity, [ms^{-1}]
W – enclosure width [m]
x – dimensional co-ordinate, [m]
y – dimensional co-ordinate, [m]

Greek symbols

α – thermal diffusivity, [m^{2}s$_{-1}$]
β – volumetric thermal expansion coefficient, [K^{-1}]
θ – non-dimensional temperature, [–]
μ – dynamic viscosity, [kgm^{-1}s^{-1}]
ρ – density, [kgm^{-1}]

Subscripts

ave – average
e – external

References

[1] Bejan, A., *Convection Heat Transfer*, 4th ed., Wiley, New York, USA, 2013
[2] Karimi, F., *et al*., Numerical Simulation of Steady Mixed Convection Around Two Heated Circular Cylinders in a Square Enclosure, *Heat Transf. Eng*., *37* (2016), 1, pp. 64-75
[3] Bergman, T., *et al*., *Fundamentals of Heat and Mass Transfer*, Jefferson: John Wiley and Sons, New York, USA, 2011
[4] Ali, O., Experimental and Numerical Investigation of Natural-convection Heat Transfer from Different Cross-Section Cylinders in a Vented Enclosure, Ph. D. thesis, Mosul University, Mosul, Iraq, 2008
[5] Kahwaji, G. Y., Samaha, M. A., Passive Natural-Convection Augmentation from Horizontal Cylinder Using a Novel Shroud-Chimney Configuration, *Journal Thermophys. Heat Transf*., *33* (2019), 4, pp. 1006-1017
[6] Rath, S., Dash, S. K., Natural-Convection in Power-Law Fluids from a Pair of Two Attached Horizontal Cylinders, *Heat Transf. Eng.*, *42* (2021), 7, pp. 627-653
[7] Ali, O., *et al.*, Numerical Investigation of Natural-Convection Heat Transfer From Circular Cylinder Inside an Enclosure Containing Nanofluids, *International Journal of Mechanical Engineering and Technology*, *5* (2014), 12, pp. 66-85
[8] Zeinab, A. M. A., *et al*., Heat Transfer Enhancement in the Complex Geometries Filled With Porous Media, *Thermal Science*, *25* (2021), 1A, pp. 39-57
[9] Nada, S. A., Said, M. A., Effects of Fins Geometries, Arrangements, Dimensions and Numbers on Natural-Convection Heat Transfer Characteristics in Finned-Horizontal Annulus, *Int. J. Thermal Science*, *137* (2018), Nov., pp. 121-137
[10] Jani, S., *et al*., Numerical Investigation of Natural-Convection Heat Transfer in a Symmetrically Cooled Square Cavity with a Thin Fin on Its Bottom Wall, *Thermal Science*, *18* (2014), 4, pp. 1119-1132
[11] Ashorynejad, H. R., *et al*., Natural-Convection in a Porous Medium Rectangular Cavity with an Applied Vertical Magnetic Field Using Lattice Boltzmann Method, *Appl. Mech. Mater*., *110-116* (2012), 1, pp. 839-846
[12] Abdulkadhim, A., *et al.*, Effect of Adiabatic Circular Cylinder on the Natural-Convection Heat Transfer Characterizes in a Porous Enclosure, *Chem. Eng. Trans*., *71* (2018), Dec., pp. 1309-1314
[13] Kahwaji, G. Y., *et al*., Experimental Investigation of Natural-Convection Heat Transfer from Square Cross-Section Cylinder in a Vented Enclosure, *Journal Univ. DUHOK Pure Eng. Sci*., *16* (2013), 1, pp. 1-10
[14] Rahmati, A. R., Tahery, A. A., Numerical Study of Nanofluid Natural-Convection in a Square Cavity with a Hot Obstacle Using Lattice Boltzmann Method, *Alexandria Eng. J*., *57* (2018), 3, pp. 1271-1286
[15] Pourmahmoud, N., *et al*., Numerical Study of Mixed Convection Heat Transfer in Lid-Driven Cavity Utilizing Nanofluid: Effect of Type and Model of Nanofluid, *Thermal Science*, *19* (2015), 5, pp. 1575-1590,
[16] Teamah, M. A., *et al*., Double Diffusive Mixed Convection Study in a Vertical Annulus at Different Aspect Ratio and Richardson Number, *Alexandria Eng. J.*, *57* (2018), 4, pp. 3559-3575

[17] Mahmoodi, M., Effect of the Inlet Opening on Mixed Convection Inside a 3-D Ventilated Cavity, *Thermal Science*, *22* (2018), 6A, pp. 2413-2424
[18] Patel, C. G., *et al*., Mixed Convective Vertically Upward Flow Past Side-by-Side Square Cylinders at Incidence, *Int. J. Heat Mass Transf.*, *127* (2018), Dec., pp. 927-947
[19] Nasseri, L., *et al*., Numerical Study of Mixed Convection in a Ventilated Square Enclosure with the Lattice Boltzmann Method, *Numer. Heat Transf. Part A Appl*., *75* (2019), 10, pp. 674-689
[20] Selimefendigil, F., *et al*., Mixed Convection in Superposed Nanofluid and Porous Layers in Square Enclosure with Inner Rotating Cylinder, *Int. J. Mech. Sci.*, *124-125* (2017), Nov., pp. 95-108
[21] Fourar, I., *et al*., Effect of Material and Geometric Parameters on Natural-Convection Heat Transfer over an Eccentric Annular-Finned Tube, *Int. J. Ambient Energy*, *42* (2019), 8, pp. 929-939
[22] Graževičius, A., *et al*., Numerical Investigation of Two-Phase Natural-Convection and Temperature Stratification Phenomena in a Rectangular Enclosure with Conjugate Heat Transfer, *Nucl. Eng. Technol*., *52* (2020), 1, pp. 27-36
[23] ***, ANSYS, Inc., ANSYS Fluent User' s Guide Releasde 15.0," ANSIS Publisher, USA, 2013
[24] ***, ANSYS, Inc., ANSYS Fluent Tutorial Guide R18, ANSYS Publisher, USA, 2018
[25] Zhu, R., *et al.*, The CFD Model Evaluation in Mixed Convection with High Richardson Number, *Int. J. Heat Mass Transf*., *149* (2020), Mar., pp. 119-133
[26] Wilcox, C., David, C., Reassessment of the Scale-Determining Equation for Advanced Turbulence Models, *AIAA J*., *26* (1988), 11, 1299

Paper submitted: November 19, 2020
Paper revised: February 1, 2021
Paper accepted: February 26, 2021